# Optimal reserve determination in the presence of A-CAES and wind, considering a stochastic approach for EVs and driver's responsibility

**MAHDI KAZEMIHA**[1] **AND KARIM AFSHAR**[1,*]

[1] *Department of electrical engineering, Imam Khomeini International University, Qazvin, Iran*
[*] *Corresponding author: afshar@eng.ikiu.ac.ir*

*Manuscript received 01 February, 2021; revised 06 March, 2021; accepted 14 March, 2021. Paper no. JEMT-2102-1278.*

**Determination of the optimal reserve requirement of clean energy systems is one of the main challenges of system scheduling. Electric vehicles (EVs) could reduce public transportation emission due to fossil fuels in the cities, although power systems confront uncertainties in the presence of EVs. Adiabatic compressed air energy storage (A-CAES) also has merits like no fossil fuel consumption, low costs, and fast start-up. It could provide various applications like energy and reserve to reduce power system costs. This paper presents a probabilistic method for optimal determining of spinning reserve in the presence of wind, A-CAES, and EVs for the day-ahead market. The optimal reserve level will determine via simultaneously optimizing the total operation cost and total expected energy not supplied. For the A-CAES facility, we consider air pressure limitations, thermal storage capacity limitations, and power output limitations. Besides, the availability, responsibility, driving patterns, and the variety of electric vehicles are also considered. The impact of incentive on system cost is analyzed either. Dc power flow is used to model the transmission flow limits. The problem is formulated as mixed-integer linear programming. Finally, the well-known 24 bus test system is used to verify the efficiency of the proposed model. At the end we found A-CAES is not suitable for participation in the reserve market and it's better to use them for peak shaving. It means the participation of A-CAES in peak shaving decreases system cost more than when it participates in the reserve market. Most of EVs will participate in reserve market and 30 percent of incentive cost will cause the optimal cost of the system.** 

***keywords:*** *Reserve capacity, adiabatic air energy storage, electric vehicles, scheduling and incentive cost optimization, low emission systems*

http://dx.doi.org/10.22109/jemt.2021.271094.1278

## NOMENCLATURE

### Sets

| | |
|---|---|
| $T$ | Set of hourly time intervals. |
| $n_{cs}$ | Set of compressors. |
| $n_{gs}$ | Set of generators. |
| $N_{gen}$ | Set of thermal units. |
| $M_{sce}$ | Set of driving patterns. |

### Parameters

| | |
|---|---|
| $l$ | Level of income($). |
| $l_m$ | Mean level of income($). |
| $ep$ | Electricity price ($/MW). |
| $\vartheta$ | Amount of incentive cost (%). |
| $I_p$ | Total incentive cost. |
| $v_a$ | The average speed of wind. |
| $v_{ci}$ | Wind turbine cut in speed. |
| $v_r$ | Wind turbine rated speed. |
| $v_{co}$ | Wind turbine cut out speed. |
| $P_{rated}$ | Wind turbine rated power. |
| $\eta_{cs}$ | A-CAES efficiency of compression stage. |
| $\eta_{gs}$ | A-CAES efficiency of generation stage. |
| $K$ | Specific heat ratio of air. |
| $R$ | Universal gas constant. |
| $T_{comp,v,i}$ | Temperature of compressor v. |
| $T_{gen,w,i}$ | Temperature of turbine w. |
| $Y_{c,k}$ | Rated pressure ratio of compressor k. |
| $Y_{g,j}$ | Rated pressure ratio of turbine j. |

$T_{er,ini}$ Initial air temperature in the air reservoir.
$c_p$ Specific heat capacity of air.
$\zeta$ Heat exchanger effectiveness.
$T_{cold}$ Temperature of cold TES working.
$T_{hot}$ Temperature of hot TES working.
$Q_{H,0}$ Initial stored heat in the heat reservoir.
$\eta, \lambda, \omega$ Cost coefficients of thermal units.
$COST_b$ Electric vehicle battery cost.
$COST_d$ Electric vehicle battery degradation cost.
$WCP$ Wind curtailment penalty price.
$life_c$ Electric vehicles battery life cycle.
$E_{st}$ Total energy storage of the battery.
$DoD$ EV battery depth of discharge.
$\bar{Q}_H$ Upper limit of thermal storage capacity.
$VOLL$ Value of loss load.
$SOCev^{min}$ Lower limit of EVs state of charge.
$SOCev^{max}$ Higher limit of EVs state of charge.
$ROCev^{min}$ Lower limit of EVs charging rate.
$ROCev^{max}$ Upper limit of EVs charging rate.

### Variables

$P_{w,average}$ Average generated power by wind.
$Pc_{es,t}$ Compressing power of A-CAES at time t.
$Pg_{es,t}$ Generating power of A-CAES at time t.
$\dot{m}_{cs,t}$ Mass flow rate in compression stage.
$\dot{m}_{gs,t}$ Mass flow rate in generating stage.
$P_{ar,t}$ Pressure of air reservoir at time t.
$x_{i,t}$ Binary variable for compressing (A-CAES).
$u_{i,t}$ Binary variable for committed generation units.
$P_{Q,C,t}$ Heat transfer power from heat exchanger during the compression of A-CAES at time t.
$P_{Q,g,t}$ Heat transfer power from heat exchanger during the expansion stage of A-CAES at time t.
$Q_{H,t}$ Stored heat in the heat reservoir.
$COST^{su}$ Startup cost of thermal units.
$COST^{shd}$ Shut down cost of thermal units.
$COST^{tu}$ Thermal units cost.
$CE_{EV}$ Cost of V2G, energy market.
$CR_{EV}$ Cost of V2G, reserve market.
$EENS_t$ Expected energy not served (MWh).
$P_t^{wc}$ Wind curtailment at hour t.
$p_{i,t}$ Total power provided by thermal unit i at hour t.
$pe_{sce,t}$ V2G power that each driving pattern provides.
$pw_t$ Wind power.
$pec_{sce,t}$ Electric vehicles charging power.
$pc_{i,t}$ A-CAES power usage in the compression stage.
$l_t$ Load at time t.

## 1. INTRODUCTION

Today many different facilities can contribute to energy markets. So scheduling energy and ancillary services has become one of the most significant concerns of system operators around the world. Spinning reserve is one of the ancillary services. The spinning reserve defines as the extra generating capacity that is provided by online generators. On the other hand, the spinning reserve is the capacity that is spinning, synchronized, and helps to balance the system withstand sudden outages of units [1]. There are deterministic and probabilistic methods to determine optimal reserve capacity. Probabilistic methods are more practical due to the stochastic nature of power systems [2]. On the other side, the existence of green-house gasses in the atmosphere could have a destructive effect on human health, the environment, and the economy [3]. Governors try to invest in renewable generation and clean transportation due to their merits like no consumption of fossil fuels and no emission. So wind energy and EV penetration are growing every day. For example, the US department of power and energy predicts that wind energy could generate 20% of the world's electricity by 2030. However, higher wind penetration causes more problems in power system operation because of the intermittent nature of wind [3]. Thus power system needs more reserve capacity to withstand unforeseen fluctuations of wind power plants, and the day-ahead operation cost increases because additional generators are committed to providing the extra reserves [1].
Likewise, the popularity of electric vehicles increases every day. Although electric cars impose more demand on the power system, they could contribute as a battery energy storage in the reserve markets to make the system more reliable in the presence of renewables and decrease system operation cost [3, 4]. Electric vehicles will be 30 percent of the transportation network by 2030 [5]. Zhao et al. proposed a model to optimize the day ahead reserve penetrating electric vehicles in the power system. The expected energy not supplied and expected energy served by EVs are two criteria that they used to optimize the spinning reserve. A three-point grid search base method is employed here to optimize the problem. The impact of immediate and smart charging on the power system is analyzed too [1]. Pavic et al. minimized power system cost penetrating renewables and electric vehicles in the system. They analyzed the impact of slow and fast EV charging on the flexibility of the power system either [6].
Some works maximized the profit of EV aggregators. The minimizing of the system cost had not been their concern. Han et al. proposed a scheduling strategy to maximize EV aggregator profit in the day ahead and real-time markets. The aggregator has participated in energy and reserve markets. The impact of the reserve call-up on aggregator revenue in the real-time market analyzed either [7]. Sortomme et al. proposed a scheduling method to maximize the profit of EV aggregator while minimizing the cost of charging for EVs. The aggregator has participated in energy and multiple ancillary services markets like regulation. The power losses are also considered in this reference [8]. Hoogvliet et al. analyzed the potential of electric vehicles in providing ancillary services such as regulation and reserve in the Netherland power system with an 8 percent grid power loss. They used four famous types of EVs in Netherland and categorized drivers into three groups [9]. Rahmani classified drivers into three social classes. Then for constant amounts of incentives, investigates the effect of each level on the hourly spinning reserve separately. A simulated annealing method is

applied to optimize the model. The charging cost formulation is different in normal conditions and contingency [10].

Some papers try to minimize the system cost and increase the reliability of the system using EVs. Zou et al. presented a multi-objective virus colony search based on fuzzy decision-making to minimize the system cost. The purpose is to satisfy the load demand by all generation units applying system constraints. Wind and EVs are considered as market participants in this reference [11]. Sadeghian et al. improved the reliability of the distribution network using electric vehicles and demand response programs. A particle swarm optimization algorithm is used in this reference. The loss of load expectation (LOLE) and expected energy not served (EENS) are used to evaluate the reliability [12].

Other than electric vehicles, different kinds of electric energy storage systems such as compressed air energy storage (CAES) [13], pumped hydro storage (PHS) [14], adiabatic compressed air energy storage (A-CAES) [15], and liquid air energy storage (LAES) [16], have attracted attention to participate in the power systems. They support the system to confront the power fluctuations due to renewables. Among all of them, A-CAES has some principal superiority over others. First of all, A-CAES storages like CAES could construct where ever we need. Compared to PHS, CAES and A-CAES have fewer construction constraints, lower costs, and higher cycle efficiency [17]. In A-CAES, recovered energy during the compression cycle is returned during the expansion cycle.

A-CAES is emission-free in comparison to CAES either. CAES uses natural gas to preheat the air stored in the reservoir. But A-CAES doesn't have fossil fuel consumption [15]. A-CAES storages like PHS and CAES is suitable for large-scale storage applications [18, 19]. In A-CAES, heat extract from the compression stage and store in a heat reservoir. So A-CAES has one air and one heat reservoir. It causes A-CAES had been higher efficiency [20, 21]. Several A-CAES systems are under development around the world. ADELE with 360 MWh storage capability, 90 MW output power, and 70 percent cycle efficiency is one of the most popular of them. 10 MW/40 MWh A-CAES near Beijing and 50 MW system in Jiangsu, China, are the other A-CAES systems under development [15].

Optimal bidding and strategies of CAES using a robust optimization approach are studied in [22]. Nojavan et al. maximized the profit of the CAES system in the presence of the uncertainty of prices [22]. Scheduling CAES in the power system is studied in [23]. Li et al. proposed a scheduling model for a combined CAES and wind system to increase the profit of the CAES facility [23]. Daneshi et al. performed a security-constrained unit commitment (SCUC) considering the advantage of energy storage system (EES) and wind. CAES is the energy storage facility in this reference. The impact of CAES on locational marginal price, peak shaving, wind curtailment, and operational cost of the power system is argued in this reference, either [24]. Ghaljehei et al. proposed stochastic security-constrained unit commitment considering CAES as EES and high penetration of wind generation. The voltage security issue of the power system is considered as a constraint in the second stage of the model [25]. Li et al. developed a joint energy and reserve scheduling model considering A-CAES, winds, and time-shifting loads. A regulation and contingency reserve capacity model for A-CAES is represented in this work [15].

The optimal reserve determination in the presence of EVs, A-CAES, and wind simultaneously is needed to show the effects of each facility in the power system. In this paper, the optimal scheduling reserve in the day-ahead market by a multistep iterating algorithm is solved. Opposed other references, for calculating EVs state of charge, we present a stochastic algorithm that considers EVs willing to participate in the markets based on their income and system incentive cost. This algorithm considers availability, the amount of consumption and battery degradation of EVs. The reserve is determined by a trade-off between expected energy not served and system cost for different amounts of spinning reserve. The reserve is calculated during optimization problem. Opposed [2], we determine reserve capacity in the presence of EVs and A-CAES, considering all uncertainties that EVs have. Finally, the minimum expense of the system has been satisfied and the effects of these participants in the reserve market are analyzed. Opposed [7, 8], we don't consider any aggregator for EVs. We look at the system as a system operator to minimize the system cost. However, their goal wasn't reserve optimization. Opposed [10], we use EENS to show the value of lost load. We also consider wind uncertainty, battery degradation cost and different groups of EVs based on a stochastic algorithm. We calculate the optimal incentive cost considering participation of all groups of people either. (Table 1) shows the basic differences between this paper and other references that this article is inspired by.

**Table 1.** Paper's highlights in comparison with other papers

| Reference | Reserve | A-CAES | EVs | Social effects | Driving patterns | Battery degradation | EENS | Wind |
|---|---|---|---|---|---|---|---|---|
| 2 | ✓ | | | | | | ✓ | ✓ |
| 4 | | | ✓ | | ✓ | | | |
| 10 | ✓ | | ✓ | ✓ | | | | |
| 15 | ✓ | ✓ | | | | | | |
| 29 | | | ✓ | | ✓ | | | |
| paper | ✓ | ✓ | ✓ | ✓ | ✓ | ✓ | ✓ | ✓ |

## 2. FORMULATION AND OPTIMIZATION OF PROBLEM

By increasing EVs in the transportation system, we can use them for supplying a part of system demand or as an ancillary services. The income of the drivers and incentive cost that system operator recommended, affect drivers decision for participating in markets. A-CAES is the other facility that can participate in the markets. These facilities can reduce the system cost by peak shaving and providing reserve. Reserve decreases load interruption costs. In the proposed model EVs and A-CAES participate in energy and reserve markets simultaneously and their effects on reserve market analyze. In subsection 2.1, the driver's financial level is modeled and three scenarios are produced based on that. In subsection 2.2 driving patterns are modeled based on [4]. Wind is modeled in subsection 2.3. A thermodynamic model of A-CAES is presented in subsection 2.4.

### A. Driver's financial level

Driver's financial level is a vital factor for the system operator. It has a significant effect on the number of drivers who participate in the markets. The responsibility of each driver depends on the incentive cost and their income. An expression to model the income of EV drivers is the Rayleigh probability density function. Rayleigh probability density function is a specific case of Weibull distribution (1).

$$f(l) = \begin{cases} a l^{b-1} e^{\frac{-a l^b}{b}} & l \geq 0 \\ 0 & Otherwise \end{cases} \quad (1)$$

In Rayleigh distribution, the shape parameter is equal to 2 (2). The mean value of employees and other people's income in each

society is known. So the C parameter in Rayleigh distribution calculates from (3).

$$f(l) = \begin{cases} \frac{l}{c^2} e^{\frac{-l^2}{2c^2}} & l \geq 0 \\ 0 & Otherwise \end{cases} \quad (2)$$

$$l_m = \int_0^\infty l f(l) dl = \int_0^\infty (\frac{l}{c^2}) e^{\frac{-l^2}{2c^2}} dl = \frac{\sqrt{\pi}}{2} c \quad (3)$$

To determine the financial level, we take samples from the Rayleigh distribution function. The social income of each driver is determined using (4).

$$f_{in}(l) = \begin{cases} low\ income & l \leq l_m \\ \text{mod}erate\ income & l_m \leq l \leq 2l_m \\ high\ income & l \geq 2l_m \end{cases} \quad (4)$$

Each level has different responsiveness to different revenue. So, the incentive amount has a significant effect on the number of EVs that participate in the markets. According to [10], the responsiveness function of each level could calculate from (5).

$$\text{Res}_{low-income,\vartheta} = 100\,(\frac{\vartheta}{100})^{0.3}$$

$$\text{Res}_{\text{mod}erate-income,\vartheta} = \vartheta$$

$$\text{Res}_{high-income,\vartheta} = 100 \exp(10(\frac{\vartheta}{100} - 1)) \quad (5)$$

### B. Driving patterns

Different drivers have different driving patterns. Electric vehicle's availability and the amount of charge that they could deliver to the power system are important factors for the system operator. According to [4], driving pattern scenarios could generate using multiplication a uniform and a normal distribution. A required energy scenario for an electric vehicle in hour t is obtained as (6).

$$cu_{ev,t} = (\delta_{EV,t} + U_{EV,t}) \times (1 + N_{EV,t}) \quad (6)$$

Where $\delta_{EV,t}$is the most expected driving patterns that have to be defined initially, applying some forecasting of EV behavior. Uniform distribution helps to model emergency usage of EVs when we define $\delta_{EV,t}$ equal to zero at first hours of the day.

### C. Wind speed modeling

Weibull distribution is used to model the behavior of wind speed. By getting some samples for wind speed from the Weibull distribution, the probability of each sector between two samples, is calculated using (7). The average value of each section uses as the average amount of wind speed to calculate the output of the wind turbine for that sector by (8). In the end, the average power of the wind turbine will calculate using (9) for each hour [26].

$$p(w) = \int_{sn1}^{sn2} f(v) dv \quad (7)$$

$$p_w(v) = \begin{cases} 0 & 0 \leq v_a \leq v_{ci}, v_{co} \leq v_a \\ p_{rated} \times \frac{(v_a - v_{ci})}{(v_r - v_{ci})} & v_{ci} \leq v_a \leq v_r \\ p_{rated} & v_r \leq v_a \leq v_{co} \end{cases} \quad (8)$$

$$P_{w,average} = \sum_w p_w(v) \times p(w) \quad (9)$$

We do this 10 times for each hour. Now we have 10 wind data for every hour. We categorize this data into three groups based on the mean value of the rated power of turbines and standard deviation of our data. If the distance between each data and mean value is smaller than the standard deviation of data, we put that in the first group. Then if the distance between each data and mean is greater than the standard deviation and that data is smaller than mean, we put that in the second group. Finally, if the distance between each data and mean is greater than the standard deviation and that data is greater than mean, we put that in the third group.The probability of each group is calculated by division of the number of group's data on the number of total data.

### D. A-CAES model

A thermodynamic model is used in this paper for A-CAES. This model is combined from CAES model and a heat reservoir model. The temperature of air reservoir is supposed to be equal to the ambient temperature. Heat loss of thermal energy storage tank is neglected. Heat exchanger is ideal. It means that hex effectiveness is supposed to be equal to 1.

The first step begins with compressing air through a series of compressors. The relationship between power consumption and mass flow rate in the compression stage and the relationship between power generation and mass flow rate in the generation stage are expressed by (10) and (11), respectively [27]. Air pressure in the air reservoir at each hour could calculate by (12). This equation shows the state of charge of A-CAES at each hour, either [27]. Heat transfer power during the compression stage, heat transfer power during the expansion stage, and the amount of heat stored in the heat reservoir calculate by (13-15), respectively [15].

$$Pc_{es,t} = \frac{\dot{m}_{cs,t}}{\eta_{cs}} \times \frac{k \times R}{k-1} \times \left[\sum_{v=1}^{n_{cs}} T_{comp,v,i} \times \left(\gamma_{c,v}^{\frac{k-1}{k}} - 1\right)\right] \quad (10)$$

$$\frac{Pg_{es,t}}{\eta_{gs}} = \dot{m}_{gs,t} \times \frac{k \times R}{k-1} \times \left[\sum_{w=1}^{n_{gs}} T_{gen,w,i} \times \left(1 - \gamma_{g,w}^{\frac{k-1}{k}}\right)\right] \quad (11)$$

$$P_{ar,t+1} = P_{ar,t} + \frac{R_g \times T_{er,t} \times \gamma}{V_{st}} \left(\dot{m}_{cs,t} \times x_{i,t} - \dot{m}_{gs,t} \times u_{i,t}\right) \quad (12)$$

$$\frac{P_{Q,C,t}}{c_p \times \zeta} = \dot{m}_{cs,t} \times \left(\sum_{v=1}^{n_{cs}} T_{comp,v,i} \times \gamma_{c,v}^{\frac{k-1}{k}} - n_{cs} \times T_{cold}\right) \quad (13)$$

$$\frac{P_{Q,g,t}}{c_p \times \zeta \times \dot{m}_{gs,t}} = \left(n_{gs} \times T_{hot} - T_{er,t} - \sum_{w=1}^{n_{gs}-1} T_{gen,w,i} \times \gamma_{g,w}^{-\frac{\gamma-1}{\gamma}}\right) \quad (14)$$

$$Q_{H,t} = Q_{H,0} + \sum_{t=1}^{T} P_{Q,C,t} - \sum_{t=1}^{T} P_{Q,g,t} \quad (15)$$

## 3. OBJECTIVE FUNCTION

The objective function minimizes the power system operation cost over the next day and formulated as (16). The first term accounts for the start-up and shut-down cost of TUs. The second and third term represents the generation cost of TUs for energy and reserve market. The fourth and fifth terms represent the cost of EVs for generating energy and reserve for each scenario of driving patterns, respectively. The sixth term of the objective function shows the expected energy not supplied of the system due to the forced outage rate of TUs and wind. The seventh term represents the cost of energy that A-CAES provide. Finally, the last term adds a penalty cost for wind accuracy to the objective function.

$$\begin{aligned}\min f_c(c_i^s) = &\sum_{t=1}^{T}\sum_{i=1}^{Ng}\left[COST_{i,t}^{su} + COST_{i,t}^{shd}\right] + \\ &\sum_{t=1}^{T}\sum_{i=1}^{Ng} P_{i,t} \times COST_{i,t}^{E} + \sum_{t=1}^{T}\sum_{i=1}^{Ng} R_{i,t} \times COST_{i,t}^{R} + \\ &\sum_{t=1}^{T}\sum_{sce=1}^{M_{sce}} CE_{EV,sce,t} + \sum_{t=1}^{T}\sum_{sce=1}^{M_{sce}} CR_{EV,sce,t} + \\ &\sum_{t=1}^{T} VOLL \times EENS_t + \sum_{t=1}^{T} COST_t^{ACAES} + \\ &\sum_{t=1}^{T} VWC \times P_t^{wc}\end{aligned} \tag{16}$$

The start-up and shut-down cost calculate from (17) and (18), respectively [10].

$$COST_{i,t}^{su} = C^{su} \times \left(1 - u_{i,t-1}\right) \times u_{i,t} \tag{17}$$

$$COST_{i,t}^{shd} = C^{shd} \times u_{i,t-1} \times \left(1 - u_{i,t}\right) \tag{18}$$

The fuel cost of each generation unit is supposed to be a quadratic polynomial function of the power 19. $\eta$,$\lambda$,and $\varpi$ are the fuel cost coefficients [10].

$$COST_{i,t}^{tu} = \eta_i \times \left(p_{i,t}\right)^2 + \lambda_i \times \left(p_{i,t}\right) + \varpi_i \tag{19}$$

The cost of providing reserve by EVs is composed of two parts, battery degradation cost, and incentive cost. In modern energy systems, the probability of spinning reserve usage is low. So we use an additional cost as electricity price just when electric vehicles participate in the energy market. According to [1], the battery degradation cost for each kind of battery calculates from (20). The cost of energy and reserve that provide by EVs are presented in (21) and (22), respectively.

$$COST_d = \frac{COST_b}{life_C \times E_{St} \times DoD} \tag{20}$$

$$CE_{ev} = E_{ev} \times \left(I_p \times \left(\frac{\vartheta}{100}\right) + COST_d + ep\right) \tag{21}$$

$$CR_{ev} = R_{ev} \times \left(I_p \times \left(\frac{\vartheta}{100}\right) + COST_d\right) \tag{22}$$

## 4. PROBLEM CONSTRAINTS

### A. Conventional unit constraints

System power balance: This constraint represents that total generating power must be equal to the total amount of consumption (23).

$$\begin{aligned}&\sum_{i=1}^{N_g} p_{i,t} + \sum_{sce=1}^{M_{sce}} pe_{sce,t} + Pw_t = L_t + \\ &\sum_{sce=1}^{M_{sce}} pec_{sce,t} + \sum_{i=A-CAES} pc_{i,t}\end{aligned} \tag{23}$$

Generation units power constraints: The maximum and minimum power of a unit at every hour are presented in (24) [10].

$$p_{\min,i} \le p_{i,t} \le p_{\max,i} \tag{24}$$

Ramp-up and ramp-down rates constraints: The possible rate of increase and decrease of the unit's output is presented in (25) and (26), respectively [10].

$$p_{i,t+1} - p_{i,t} \le RU_i \tag{25}$$

$$p_{i,t} - p_{i,t-1} \le RD_i \tag{26}$$

Min up time and min down time constraints: The minimum uptime and minimum downtime of each generation unit after a change in the status of the unit are presented in (27) and (28), respectively [10].

$$ontime_{i,t} \ge MUT_i \tag{27}$$

$$offtime_{i,t} \ge MDT_i \tag{28}$$

### B. Transmission lines constraints

Lines capacity constraints: The maximum power that passes through lines is expressed by (29) [30].

$$-p_{bn}^{\max} \le p_{bn} \le p_{bn}^{\max} \tag{29}$$

Transferable power from each bus: The power that each bus could inject to other busses is expressed by (30). This power is calculated by submission the power consumption from power generation at each bus.

$$\begin{aligned}&\sum_{i=1}^{N_{gen}} P_{bus,i,t} + \sum_{sce=1}^{M_{sce}} P_{bus,sce,t} + Pw_{bus,t} + Pacaes_{bus,t} \\ &-L_{bus,t} - \sum_{sce=1}^{M_{sce}} Pec_{bus,sce,t} - Pc_{bus,t} = Pbn_{bus,node,t}\end{aligned} \tag{30}$$

### C. A-CAES constraints

Generating power constraint of A-CAES: The maximum and minimum power of an A-CAES unit in generation mood at every hour are presented in (31). u(i,t), is a binary variable that shows generation mood is working [15].

$$Pg_{es,\min} \times u_{i,t} \le Pg_{es,i,t} \le Pg_{es,\max} \times u_{i,t} \tag{31}$$

Compressing power constraint of A-CAES: The maximum and minimum power that an A-CAES unit uses to compress air into the air reservoir is calculated by (32). $x_{i,t}$ is a binary variable that shows the compression mood is working [15].

$$Pc_{es,\min} \times x_{i,t} \le Pc_{es,i,t} \le Pc_{es,\max} \times x_{i,t} \tag{32}$$

Non simultaneity of compressing and generating modes: An A-CAES unit couldn't work in generating and compressing mood simultaneously. This constraint is presented by (33) [15].

$$x_{i,t} + u_{i,t} \le 1 \qquad \forall i \equiv A - CAES \tag{33}$$

Air pressure limitation: Air pressure limitation in the air reservoir is presented in (34) [15].

$$P_{ar,\min} \le P_{ar,t} \le P_{ar,\max} \tag{34}$$

Capacity of heat reservoir: The maximum thermal capacity of the heat reservoir is shown by (35) [15].

$$0 \le Q_{H,t} \le \overline{Q}_H \tag{35}$$

### D. Electric vehicles constraints

Electric vehicles state of charge constraint: The state of charge range of each electric vehicle is presented by (36) [29].

$$SOC_{ev}^{\min} \le SOC_{ev} \le SOC_{ev}^{\max} \tag{36}$$

Charging rate constraint: EVs charging rate limitation is presented by (37) [29].

$$ROC_{ev}^{\min} \le ROC_{ev} \le ROC_{ev}^{\max} \tag{37}$$

Maximum V2G power: The maximum power that each EV could deliver to the grid is calculated by (38). $P_x^{EVr}$ is the rated power of battery for each EV [10].

$$P_{ev} + R_{ev} \le \frac{SOC_{ev} - P_{consume} - SOC_{ev}^{\min}}{100} \times \frac{P_x^{EV_r}}{1000} \tag{38}$$

## 5. CALCULATION OF EXPECTED ENERGY NOT SUPPLIED AND RESERVE DETERMINATION METHOD

The expected energy curtailed can obtain from the installed capacity of generating units and load. The probability of forced outage rate of each generation units, the amount of demand, and the spinning reserve capacity that each generation unit provides, could show the amount of expected energy not served. Forced outage rate defines as the probability of failure of a generator, and it is usually measured as a ratio of failure hours to total service hours. The maximum EENS calculates from the capacity outage probability table (COPT). The probability of a random outage event of a single generator can be shown by (39). The amount of EENS at each hour could be formulated as (40) [2].

$$\Pr_{i,t} = u_{i,t} \times U_i \prod \left( (1 - u_{j,t}) \times U_j \right) \tag{39}$$

$$EENS_t = \left\{ \sum_{i=1}^{G} \left[ P_{i,t} + r_{i,t} \right] - \left[ r_t \right] \right\} \times \Pr_{i,t} \tag{40}$$

An iterative multistep algorithm is proposed in this paper to determine the optimal reserve capacity. At first, the amount of spinning reserve capacity is equal to zero. The unit commitment (UC) problem is solved, the COPT is created, and the maximum expected energy not served is determined. Then till reserve capacity is lower than the maximum EENS, it will be added 1 megawatt to the reserve capacity and solve the optimization problem to minimize the system cost. In each iteration system cost will update if is it lower than previous iteration. The algorithm is stopped when the mentioned criterion convergence is achieved. The algorithm is shown in fig. 1. The GAMS software is used to minimize the system cost. The optimization problem is solved using MILP by means of CPLEX solver.

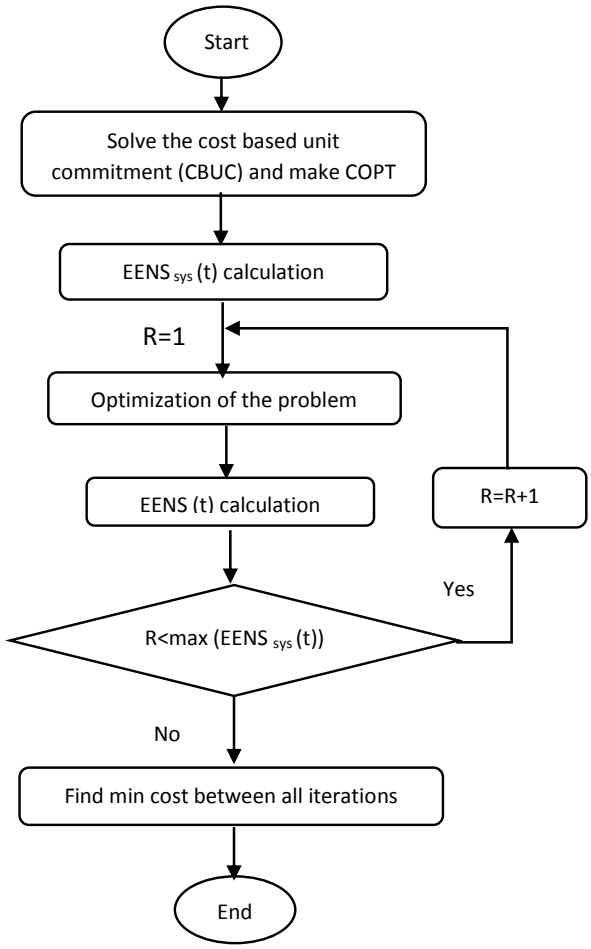


**Fig. 1.** Multistep iteration algorithm for reserve determination.

## 6. SOLVING METHOD

As it can be seen, there are some complicated nonlinear relationships between the equations of this problem. So, the optimal scheduling problem will be mixed-integer nonlinear programming (MINLP). The MINLP needs a lot of time to find the optimal point, and the performance is affected by the starting points. Compared to MINLP, mixed-integer linear programming (MILP) obtain a good result with less computational time and complexity. So we use a piecewise linear approximation for each unit's cost curve. For A-CAES, the temperature in the air reservoir is set to be equal to the initial air temperature [17]. Now equations (12) and (14) in 2.4 section are linear.

## 7. CASE STUDY

### A. Setting and assumptions

IEEE 24 bus system is used to represent the performance of the model. Fig. 2 illustrates the diagram of the 24 bus system. The wind farm is located on bus 3 [15]. A-CAES unit is located near the wind farm [15]. The branch data for the IEEE RTS 24-bus network and the generation unit's data in this network are based on [28]. Cost coefficients are shown in Table 2. Load data are shown in Fig. 3, either [28].

For analyzing the impact of A-CAES and EVs, three scenarios are considered. At first, UC and reserve determination is done for conventional units considering wind uncertainty. Three data

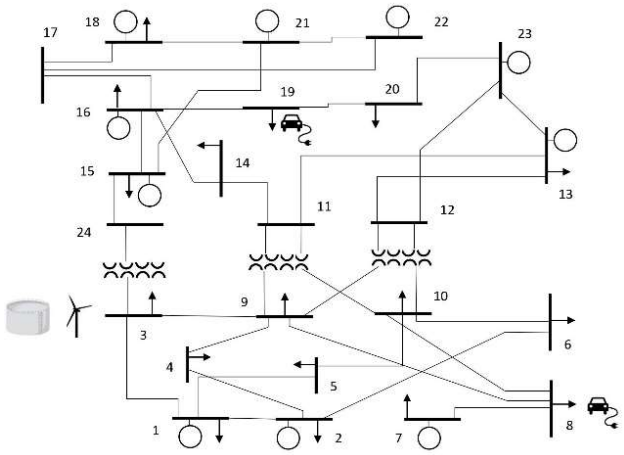


**Fig. 2.** One-line diagram of IEEE 24 bus system.

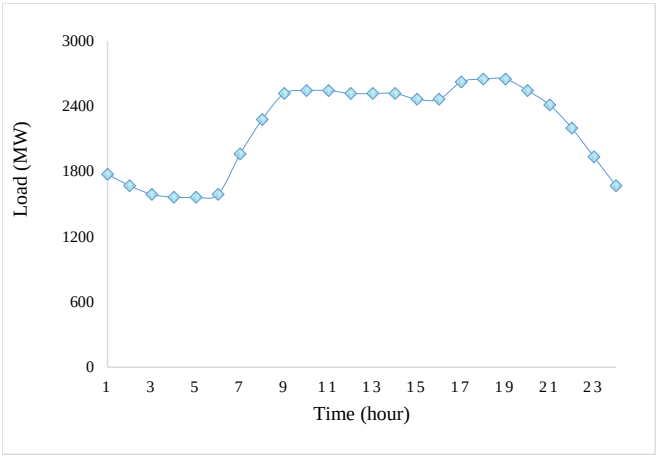


**Fig. 3.** Load power forecast curves [28].

**Table 2.** Cost coefficients of thermal units

| | G1 | G2 | G3 | G4 | G5 | G6 | G7 | G8 | G9 | G10 | G11 | G12 |
|---|---|---|---|---|---|---|---|---|---|---|---|---|
| $\eta$ | 0/04 | 0/05 | 0/04 | 0/04 | 0/05 | 0/05 | 0/06 | 0/06 | 0/06 | 0/08 | 0/06 | 0 |
| $\lambda$ | 39/6 | 39/6 | 46/5 | 46/5 | 58/2 | 55/7 | 53/7 | 69/7 | 78/9 | 80/1 | 85/31 | 0 |
| $\omega$ | 382 | 349 | 400 | 405 | 372 | 329 | 332 | 340 | 325 | 315 | 310 | 0 |

produce for wind power. Then in the second scenario, the problem is solved by penetrating the A-CAES unit to show the impact of A-CASE participation in the market. The A-CAES parameters are shown in Table 3 [15]. In the last scenario, EVs are one of the participants in the reserve market. A scenario-based algorithm is proposed to calculate the state of charge of EVs and the available power (Fig. 4). Each driver has a different income and responsiveness to the amount of incentive, as shown in part 1 of Fig. 4. This issue has effects on the number of EVs participation in the markets. So, system operators must have this information for decision making with the least error. Each driver uses different types of EVs. EV categories are according to the number of EV sales in 2017. The EV brand's information is in Table 4 [29]. These categories are shown in part 2 of Fig. 4. According to [4], ten scenarios are produced from three different driving patterns. Table 5 shows the probability of each of them [4]. These scenarios are shown in part 3 of Fig. 4.

The system operator needs the EV battery's characteristics like

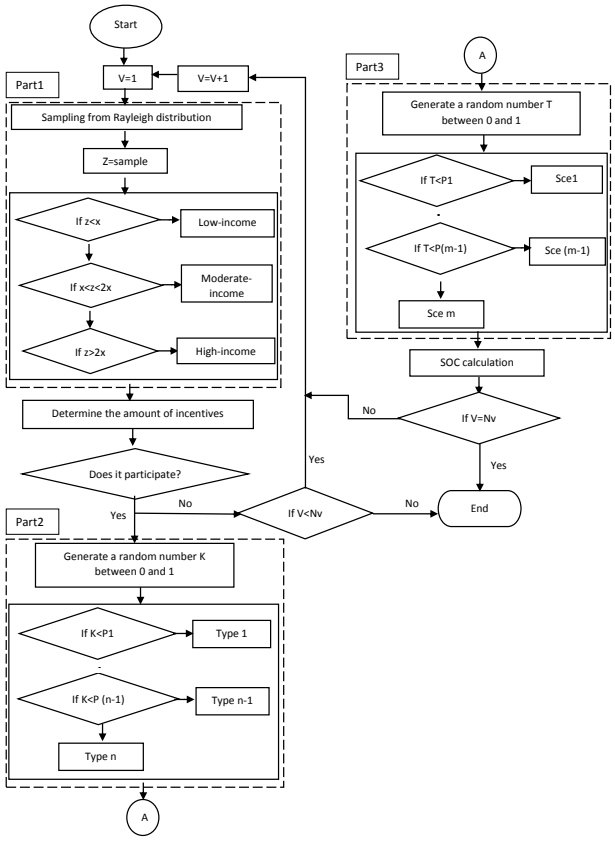


**Fig. 4.** Generating scenario considering income level, uncertainty of EVs participation, type of EVs and driving patterns.

**Table 3.** Scheduling parameters of A-CAES [15]

| Parameters | value | parameters | value |
|---|---|---|---|
| Max/Min compressing power (MW) | 100/60 | Air reservoir volume (m^3) | $4.8 * 10^5$ |
| Max/Min generating power (MW) | 100/40 | Cost coefficient ($/MW) | 2/5 |
| Number of compressors/turbines | 4 | Cold/hot TES working temperature (K) | 293/363 |
| Compression/expansion ratio | 2.75/2.4 | Max/min pressure in air reservoir (bar) | 55/40 |
| Efficiency | 85% | Initial temperature in air reservoir (K) | 316 |
| Thermal storage capacity (MJ) | $2 * 10^6$ | Initial pressure in air reservoir (bar) | 47/5 |
| Average input temperature of the air reservoir (K) | 323 | Initial stored heat in heat reservoir (MJ) | $1 * 10^6$ |
| Ramp up/ down (MW/h) | 40 | | |

**Table 4.** Electric vehicles 2017 sales data [29]

| EV brand | Selling percentage (%) | Battery capacity (kWh) | Maximum charging rate (kW) |
|---|---|---|---|
| Nissan Leaf | 25/52 | 40 | 11/5 |
| Tesla S | 21/81 | 100 | 17/2 |
| Tesla X | 18/64 | 100 | 17/2 |
| Renault Zoe | 15 | 41 | 20 |
| Other EVs | 19/03 | 25 | 12/5 |

cycle life, depth of discharge, and cost of each battery. EV batteries cycle life depends on the depth of discharge. Li-ion batteries have 1000000 cycle life at 3 percent depth of discharge and 3000 cycle life at 100 percent depth of discharge. In this paper, the EV batteries have 90 percent depth of discharge and 10000 cycle life. The cost of each EV battery is calculated based on the battery capacity. The battery cost is 200 dollars per kilowatt based on the latest data. The energy cost for EVs charging is equal to the mean value of generation cost and 70 dollars per megawatt. In

**Table 5.** Probability of each scenario [4]

| Scenario | Probability |
|---|---|
| 1 | 0/09 |
| 2 | 0/05 |
| 3 | 0/057 |
| 4 | 0/06 |
| 5 | 0/077 |
| 6 | 0/12 |
| 7 | 0/13 |
| 8 | 0/083 |
| 9 | 0/183 |
| 10 | 0/15 |

the end, to analyze the impact of the incentive on the system operating cost, the third scenario is repeated for 10, 20, and 40 percent of the maximum amount of incentive. Results show that the amount of the incentive has a significant effect on EVs participation and system cost. The maximum amount of incentive cost is 100 dollars. Mean level of people income is equal to 3000 dollars in this study. The total number of electric vehicles (Nv) in the case study is equal to 10000.

## B. Results and analysis

### *B.1. Case 1:Scheduling of the power system with A-CAES*

The amount of spinning reserve and the expected energy not served in the system considering A-CAES are shown in Fig. 5. Energy generation, energy consumption, and reserve provision of the A-CAES are shown in Fig. 6. As it can be seen, A-CAES helps system to provide more spinning reserve with lower cost. A-CAES doesn't participate in the reserve market, but in the energy market by charging at off-peak periods and discharging at peak periods decreases the total cost of the system and increases the total amount of spinning reserve of the power system that provided by thermal units (Table 6). A-CAES causes that unit 11 turn on at hour 8 instead of 7 and unit 10 turn off at hour 21 instead of 22. In other words, it can shift load from peak to valley as it can be seen in (Table 7).

**Table 6.** Power system cost with and without A-CAES

| | Without A-CAES | With A-CAES |
|---|---|---|
| Total cost (M$) | 3/251 | 3/2472 |
| reserve (MW) | 2036/36 | 2187/04 |

### *B.2. Case 2:Scheduling of the power system with A-CAES considering EV participation (10 percent of incentives)*

The generation schedules are shown in Fig. 7. G1 and G2 supply most demand because of their higher capacity and lower cost. The negative part of the A-CAES curve at the early hours of the day shows the power consumption of this storage system. The total spinning reserve and expected energy not supplied by the system are shown in Fig. 8. EVs decrease the total EENS of the system by providing additional spinning reserve at peak

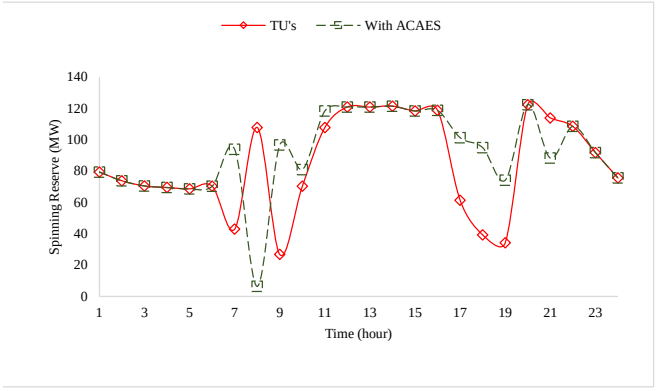


(a)

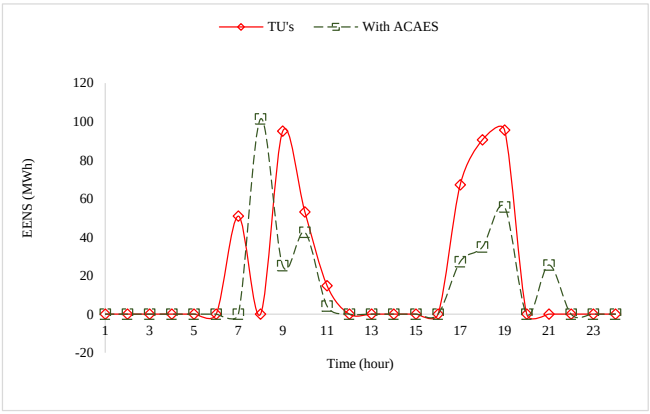


(b)

**Fig. 5.** (a) Optimal spinning reserve and (b) expected energy not served in the presence of A-CAES at each hour.

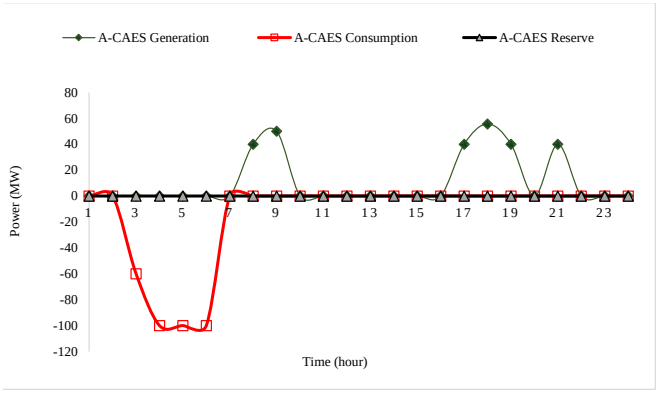


**Fig. 6.** Energy generation, energy consumption, and reserve provision of the A-CAES.

periods. Fig. 9 shows the spinning reserve capacity that each scenario of EV's provides for the power system by 10 percent of the total incentive. The ability of electric vehicles to provide reserve at peak load periods is evident in Fig. 9. Results show that the presence of EV's decrease in total system cost (Table 8). Most of EVs participate in the reserve market because it is more economical for the system in the proposed model.

### *B.3. Impact of incentive on EV's and system cost*

To analyze the impact of EVs on system cost, we considered three amounts of incentive and optimized the problem. Like 10

**Table 7.** G10 and G11 scheduling before and after A-CAES participation

| Generation unit | Before A-CAES participation |
|---|---|
| G10 | 000000011111111111111000 |
| G11 | 000000111111111111111100 |
| Generation unit | After A-CAES participation |
| G10 | 000000001111111111110000 |
| G11 | 000000011111111111111100 |

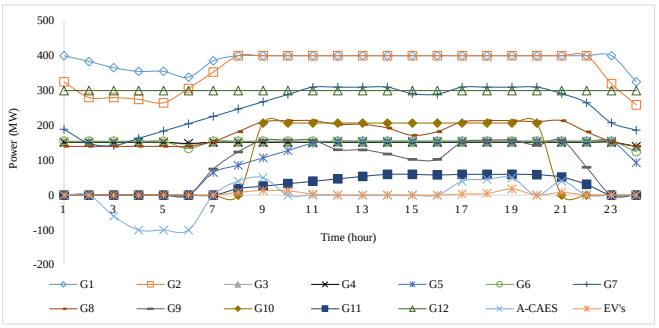


**Fig. 7.** Generation schedules in the presence of A-CAES and EVs (10% incentive).

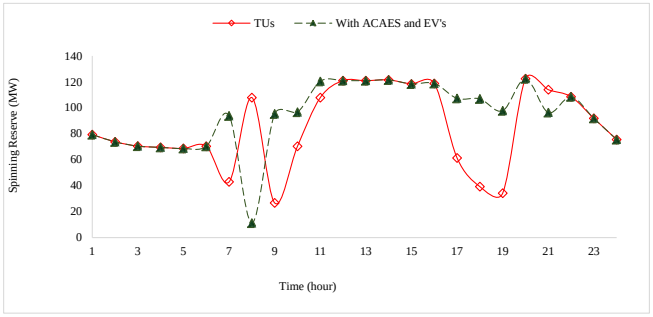


(a)

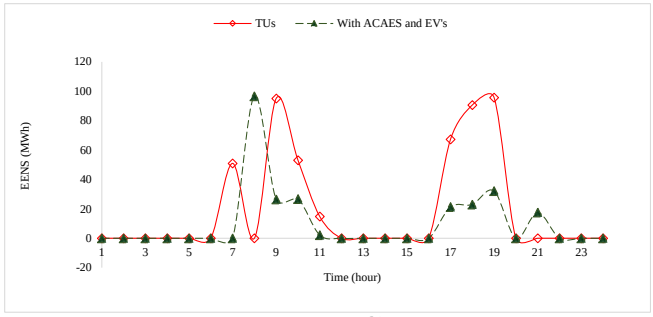


(b)

**Fig. 8.** (a) Optimal spinning reserve and (b) expected energy not served in the presence of A-CAES and EVs at each hour.

percent, the presence of EVs and A-CAES could decrease the total EENS by increasing the reserve.

Fig. 10 shows the number of electric vehicles that participate in the reserve market in each scenario of driving patterns for different amounts of incentives. As expected, the EVs number increases by increasing the incentive cost. The incentive cost

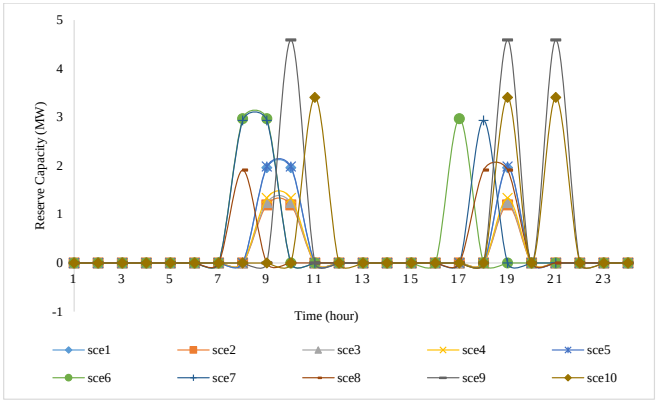


**Fig. 9.** Spinning reserve capacity that each driving pattern of EVs provide at each hour after scheduling (10% incentive).

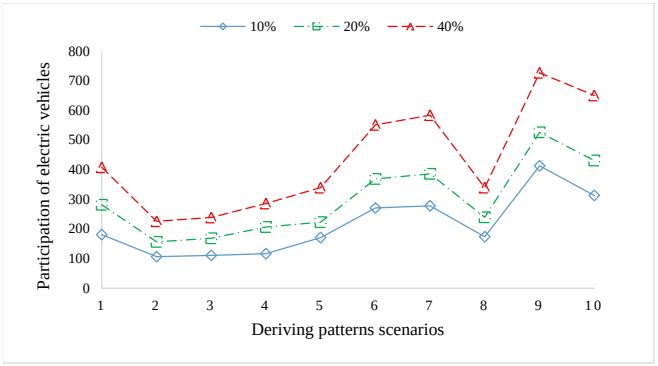


**Fig. 10.** Participation of EVs for different amount of incentive at each scenario.

**Table 8.** Power system cost of third scenario in the presence of A-CAES and EVs (10% incentive)

| | Without EVís | With EVís |
|---|---|---|
| Total cost (M$) | 3/2472 | 3/2424 |
| reserve (MW) | 2187/04 | 2257/64 |

has a significant effect on low-income people's participation in the reserve market. Unlike, the impact of the incentive cost on high-income people is almost negligible. The presence of EVs in the reserve market could decrease system costs. The total system cost for all scenarios is shown in Table 9. The total cost of the power system for the third scenario is shown for three different amounts of incentive costs. The increase in the incentive up to 20 percent decreases total system cost, but the increase in that up to 40 percent in addition to the EVs number, increases total system cost. So the amount of incentive is one of the main factors for the system operator because incentive costs is important for minimizing the objective function.

### *B.4. Impact of incentive on the total system cost*

The sensitivity analysis is done to show the impact of incentive on the system cost. Since we define incentive as an input, we need this analysis to see the impact of the input on the output. This sensitivity analyses helps system operator to determine the optimal incentive cost for electric vehicles. As it can be seen

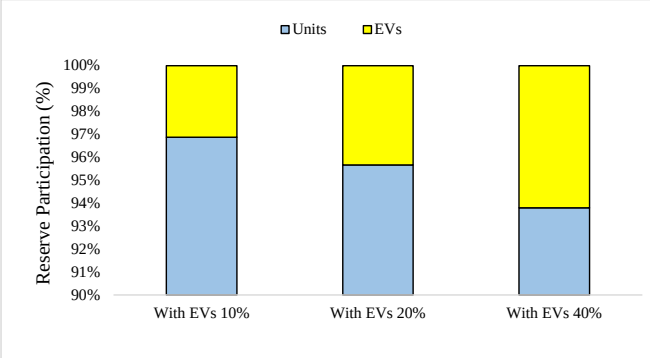


**Fig. 11.** Participation of EVs in reserve market for different amount of incentives.

**Table 9.** System cost for different scenarios

| Cost (M$) | Participants |
|---|---|
| 3/3172 | TUs |
| 3/251 | TUs + Wind |
| 3/2472 | TUs + Wind + A-CAES |
| 3/2424 | TUs + Wind + A-CAES + EV (10%) |
| 3/2415 | TUs + Wind + A-CAES + EV (20%) |
| 3/2418 | TUs + Wind + A-CAES + EV (40%) |

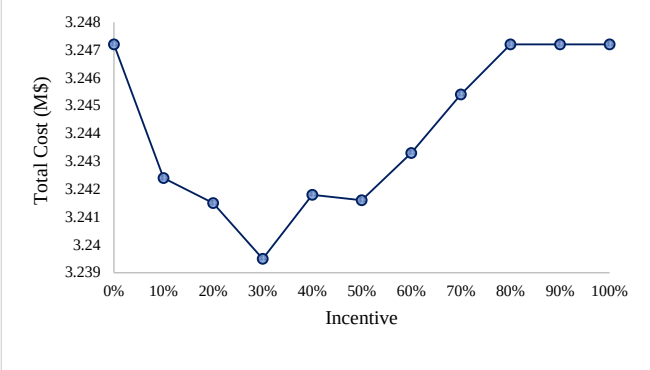


**Fig. 12.** Total power system cost for different amounts of incentives.

in Fig. 12, 30% of incentive cause the minimum system cost. Minimum system cost will be 3.2395 M$

#### *B.5. Impacts of A-CAES maximum limits on reserve and total cost of the system*

We change the maximum compressing and generating power of the A-CAES in the same time from 60% to 110% of their amount. Fig. 13 shows that the amount of system cost will decrease by applying these changes to such limits of A-CAES. Fig. 14 shows the total amount of spinning reserve that is scheduled for 24 hour by changing these limits. The incentive cost of system for EVs is equal to 30% in this part.

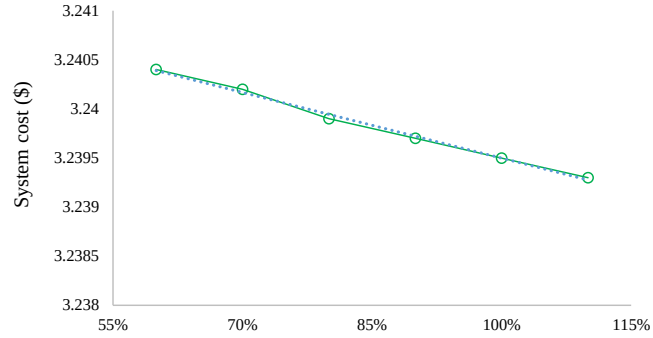


**Fig. 13.** Total power system cost for different amounts of maximum limits of A-CAES.

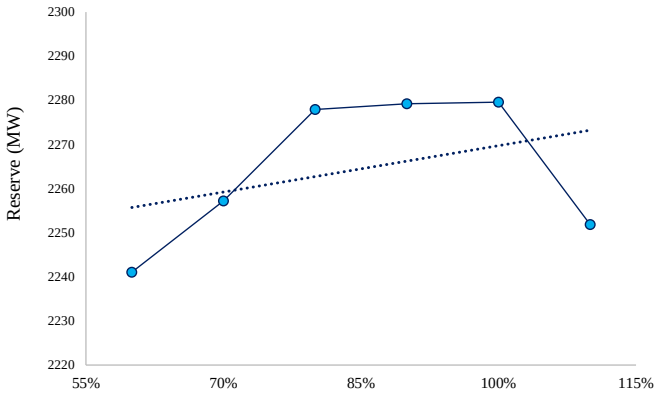


**Fig. 14.** Total reserve for different amounts of maximum limits of A-CAES.

## 8. CONCLUSION

This paper presents an optimal reserve determination model for new power and transportation systems. Wind, EVs, and A-CAES are three emission-free facilities that participate in the energy and reserve markets simultaneously. The goal is to minimize total system cost as a system operator. The impact of each facility on the reserve market and total system cost is analyzed. A new scenario base algorithm is presented to show the EV uncertainties like electric vehicle participation based on the amount of income and incentive cost, driving patterns, and different size of EV batteries. The EENS is the criterion that is used to determine the optimal reserve of the power system. In the end, it is found that EVs and A-CAES as emission-free components could decrease the system cost in addition to the amount of pollution and increase the system reliability. Since the EVs participation in reserve market has lower cost for system operator in the present model, most of the EV capacity is scheduled for reserve market. We found that A-CAES isn't suitable for reserve because the power of A-CAES is scheduled just for the energy market. It means the participation of A-CAES in peak shaving decreases system cost more than when it participates in the reserve market. The efficiency of A-CAES is equal to 73% in this study that shows the model is practical. The income of EVs had a significant effect on their willingness for participating in the market. We need different amounts of incentive for forcing them to participate in the market. We found the optimal incentive cost for all social levels is 30% in this case study. The increasing in the capacity of compressing and generating of A-CAES units could decrease

the system cost either. This increasing could make system more reliable to some extent.

## REFERENCES


1. J. Zhao, C. Wan, Z. Xu, and K. P. Wong, "Spinning Reserve Requirement Optimization Considering Integration of Plug-In Electric Vehicles," in IEEE Transactions on Smart Grid, vol. 8, no. 4, pp. 2009-2021, 2017.
2. M. MohammadGholiha, K. Afshar, and N. Bigdeli. "Optimal Reserve Determination Considering Demand Response in the Presence of High Wind Penetration and Energy Storage Systems," Iran J Sci Technol Trans Electr Eng, 44, 1403–1428, 2020.
3. E. Mirmoradi, and H. Ghasemi. "Market clearing with probabilistic spinning reserve considering wind uncertainty and electric vehicles," Trans. Electr. Energ. Syst, 26: 525– 538, 2016.
4. M. Alipour, B. Mohammadi-Ivatloo, M. Moradi-Dalvand, and K. Zare, "Stochastic scheduling of aggregators of plug-in electric vehicles for participation in energy and ancillary service markets," Energy, vol. 118, pp. 1168-1179, 2017.
5. M. Noori, and O. Tatari, "Development of an agent-based model for regional market penetration projections of electric vehicles in the United States," Energy, vol. 96, pp. 215-230, 2016.
6. I. Pavić, T. Capuder, and I. Kuzle, "A Comprehensive Approach for Maximizing Flexibility Benefits of Electric Vehicles," in IEEE Systems Journal, vol. 12, no. 3, pp. 2882-2893, 2018.
7. B. Han, S. Lu, F. Xue, and L. Jiang, "Electric vehicle charging and discharging scheduling considering reserve call-up service," 2017 International Smart Cities Conference (ISC2), Wuxi, pp. 1-6, 2017.
8. E. Sortomme, and M. A. El-Sharkawi, "Optimal Scheduling of Vehicle-to-Grid Energy and Ancillary Services," in IEEE Transactions on Smart Grid, vol. 3, no. 1, pp. 351-359, 2012.
9. T.W. Hoogvliet, G.B.M.A. Litjens, and W.G.J.H.M. van Sark, "Provision of regulating- and reserve power by electric vehicle owners in the Dutch market," Applied Energy, vol. 190, pp. 1008-1019, 2017.
10. M. Rahmani-Andebili. "Spinning Reserve Capacity Provision by the Optimal Fleet Management of Plug-In Electric Vehicles Considering the Technical and Social Aspects." In: Planning and Operation of Plug-In Electric Vehicles. Springer, Cham, 2019.
11. Y. Zou, J. Zhao, D. Ding, F. Miao, and B. Sobhani. "Solving dynamic economic and emission dispatch in power system integrated electric vehicle and wind turbine using multi-objective virus colony search algorithm," Sustainable Cities and Society, vol. 67, 2021.
12. O. Sadeghian, M. Nazari-Heris, M. Abapour. S.Taheri, and K. Zare. "Improving reliability of distribution networks using plug-in electric vehicles and demand response," J.Mod. Power syst. Clean Energy, vol. 7, pp. 1189-1199, 2019.
13. H. Park, and R. Baldick, "Integration of compressed air energy storage systems co-located with wind resources in the ERCOT transmission system," International Journal of Electrical Power & Energy Systems, vol. 90, pp. 181-189, 2017.
14. M. Chazarra, J. I. Pérez-Díaz, and J. García-González, "Optimal Joint Energy and Secondary Regulation Reserve Hourly Scheduling of Variable Speed Pumped Storage Hydropower Plants," In: IEEE Transactions on Power Systems, vol. 33, no. 1, pp. 103-115, 2018.
15. Y. Li, S. Miao, S. Zhang, B. Yin, X. Luo, M. Dooner, and J. Wang, "A reserve capacity model of AA-CAES for power system optimal joint energy and reserve scheduling, " International Journal of Electrical Power & Energy Systems, vol. 104, pp. 279-290, 2019.
16. A. Sciacovelli, A. Vecchi, and Y. Ding, "Liquid air energy storage (LAES) with packed bed cold thermal storage – From component to system level performance through dynamic modelling," Applied Energy, vol. 190, pp. 84-98, 2017.
17. A. Benato, and A. Stoppato, "Energy and cost analysis of an Air Cycle used as prime mover of a Thermal Electricity Storage," Journal of Energy Storage, vol. 17, pp. 29-46, 2018.
18. W. He, J. Wang, and Y. Ding, "New radial turbine dynamic modelling in a low-temperature adiabatic compressed air energy storage system discharging process," Energy Conversion and Management, vol. 153, pp. 144-156, 2017.
19. M. Raju, and S. Kumar Khaitan, "Modeling and simulation of compressed air storage in caverns: A case study of the Huntorf plant," Applied Energy, vol. 89, no 1, pp. 474-481, 2012.
20. X. Luo, J. Wang, C. Krupke, Y. Wang, Y. Sheng, J. Li, Y. Xu, D. Wang, S. Miao, and H. Chen, "Modelling study, efficiency analysis and optimization of large-scale Adiabatic Compressed Air Energy Storage systems with low-temperature thermal storage," Applied Energy, vol. 162, pp. 589-600, 2016.
21. N. Hartmann, O. Vöhringer, C. Kruck, and L. Eltrop, "Simulation and analysis of different adiabatic Compressed Air Energy Storage plant configurations," Applied Energy, vol. 93, pp. 541-548, 2012.
22. S. Nojavan, A. Najafi-Ghalelou, M. Majidi, and K. Zare, "Optimal bidding and offering strategies of merchant compressed air energy storage in deregulated electricity market using robust optimization approach," Energy, vol. 142, pp. 250-257, 2017.
23. Y. Li, S. Miao, X. Luo, and J. Wang, "Optimization model for the power system scheduling with wind generation and compressed air energy storage combination," 2016 22nd International Conference on Automation and Computing (ICAC), Colchester, pp. 300-305, 2016.
24. H. Daneshi and, A. K. Srivastava, "Security-constrained unit commitment with wind generation and compressed air energy storage," in IET Generation, Transmission & Distribution, vol. 6, no. 2, pp. 167-175, 2012.
25. M. Ghaljehei, A. Ahmadian, M. Aliakbar Golkar, T. Amraee, and A. Elkamel, "Stochastic SCUC considering compressed air energy storage and wind power generation: A techno-economic approach with static voltage stability analysis," International Journal of Electrical Power & Energy Systems, vol. 100, pp. 489-507, 2018.
26. Y. M. Atwa, and E. F. El-Saadany, "Probabilistic approach for optimal allocation of wind-based distributed generation in distribution systems," in IET Renewable Power Generation, vol. 5, no. 1, pp. 79-88, January 2011.
27. LI, R., CHEN, L., YUAN, T. et al. "Optimal dispatch of zero-carbon-emission micro Energy Internet integrated with non-supplementary fired compressed air energy storage system," J. Mod. Power Syst. Clean Energy, vol. 4, pp. 566–580 2016.
28. C. Ordoudis, P. Pinson, J.M. Morales González, and M. Zugno. "An Updated Version of the IEEE RTS 24-Bus System for Electricity Market and Power System Operation Studies," Technical University of Denmark.
29. P. Aliasghari, B. Mohammadi-Ivatloo, M. Alipour, M. Abapour, and K. Zare, "Optimal Scheduling of Plug-in Electric Vehicles and Renewable Micro-grid in Energy and Reserve Markets Considering Demand Response Program," Journal of Cleaner Production, vol. 186, pp. 293-303, 2018.
30. A. Soroudi, "Power system optimization modeling in GAMS", Dublin, Springer International Publishing, 2017.